Superconducting Charge Qubit

27.11.09 | SQ1

Single-Electron-Transistor

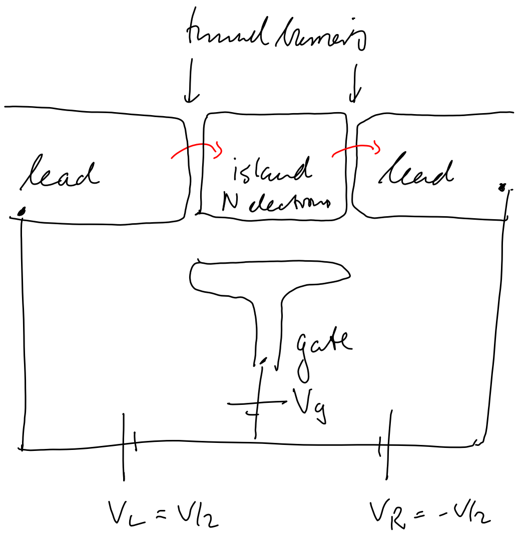

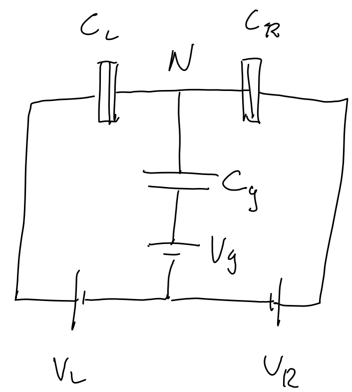

SQ2

Charging energy:

Electrostatic work required to add N electrons, total charge $Q = Ne$ $(e<0)$, to initial random charge Q_0:

$$E(N) = E_c\left(N - N_g\right)^2 ,$$

$$N_g = -\frac{eV_g}{2E_c} \qquad \text{(gate-tunable constant)}$$

$$E_c = \frac{e^2}{C} = \text{charging energy} = \text{typically } 100\text{ mK to } 100\text{ K}$$

(100 mK for large island, 100 K for small island)

, $C = C_L + C_R + C_g$ ($\sim$ area of junctions) small for small junctions)

SQ3

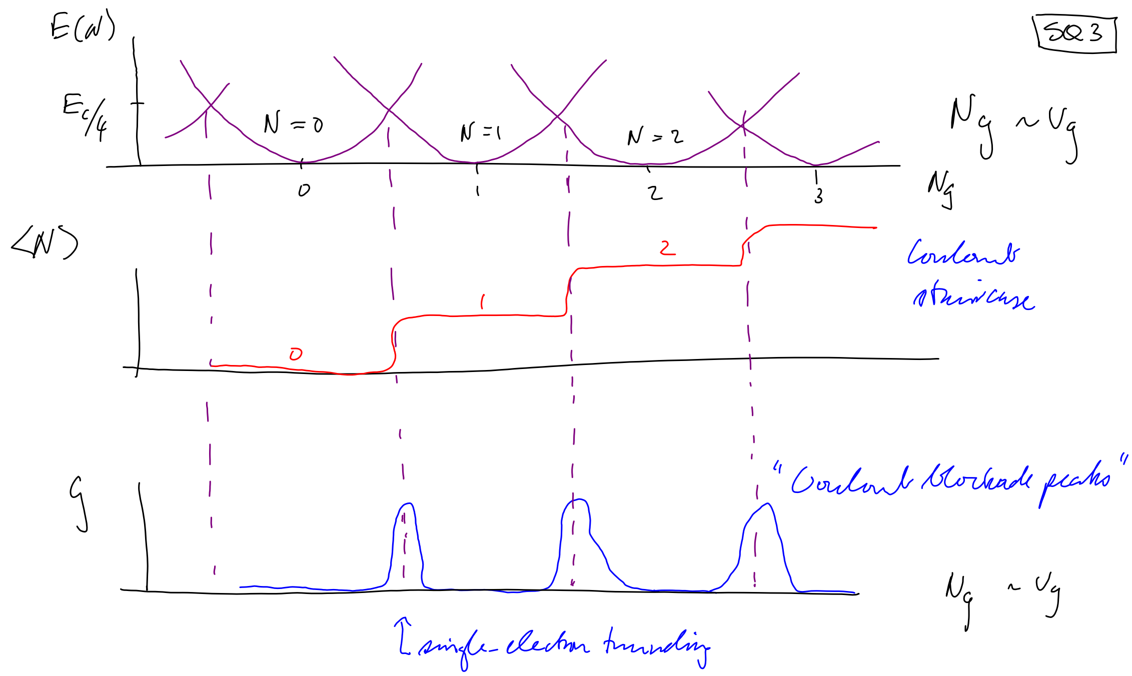

Transport possible only at intersections of parabolas,

where $E(N) = E(N+1)$ "e-periodicity"

For superconducting islands: energy penalty Δ for odd grains! SQ4

If $\Delta > E_c$: "2e-periodicity".

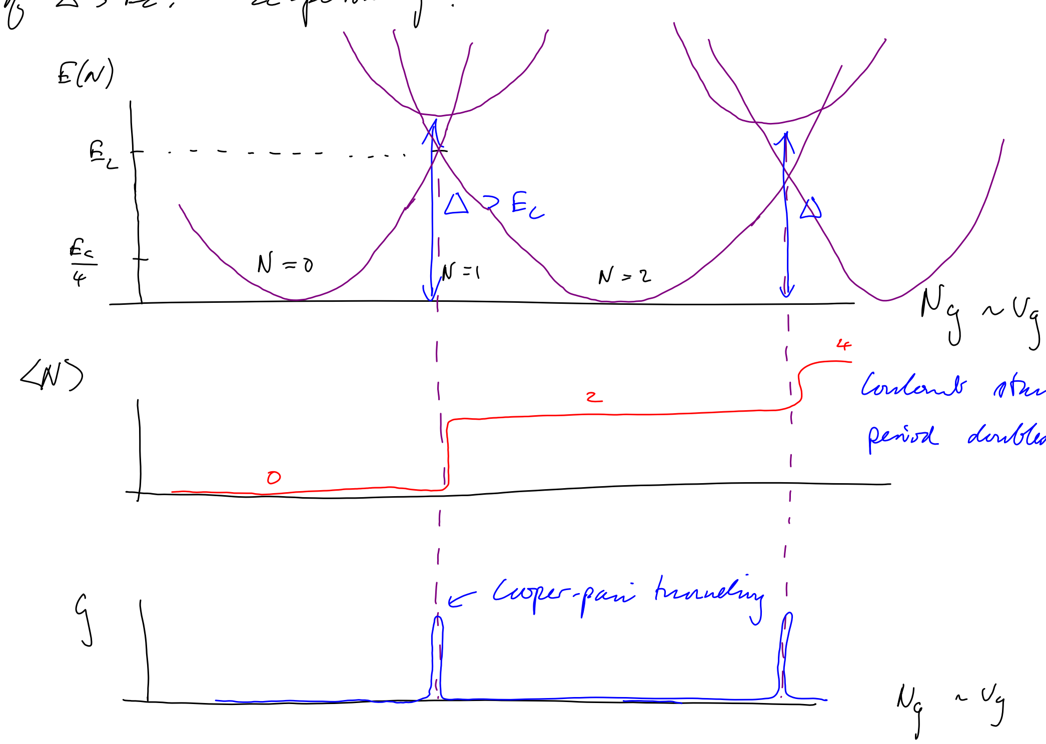

SQ5

Cooper pair box

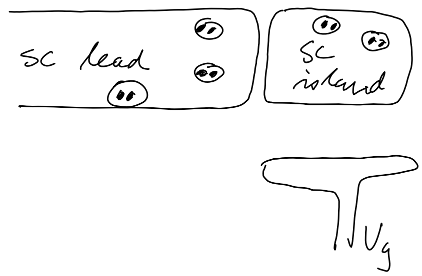

$$H_{\text{island}} = E_c (N - N_g)^2 + E_J \sum_{N=-\infty}^{\infty} |N\rangle\langle N+2| \qquad (\text{for } \Delta > E_c)$$

charging energy — Cooper pair tunneling between island and lead

E_J = "Josephson coupling" (describes tunneling strength)

E_J = tunable by magnetic field if island is part of a loop, and flux through loop is tuned.

SQ6

Focus on one degeneracy point:

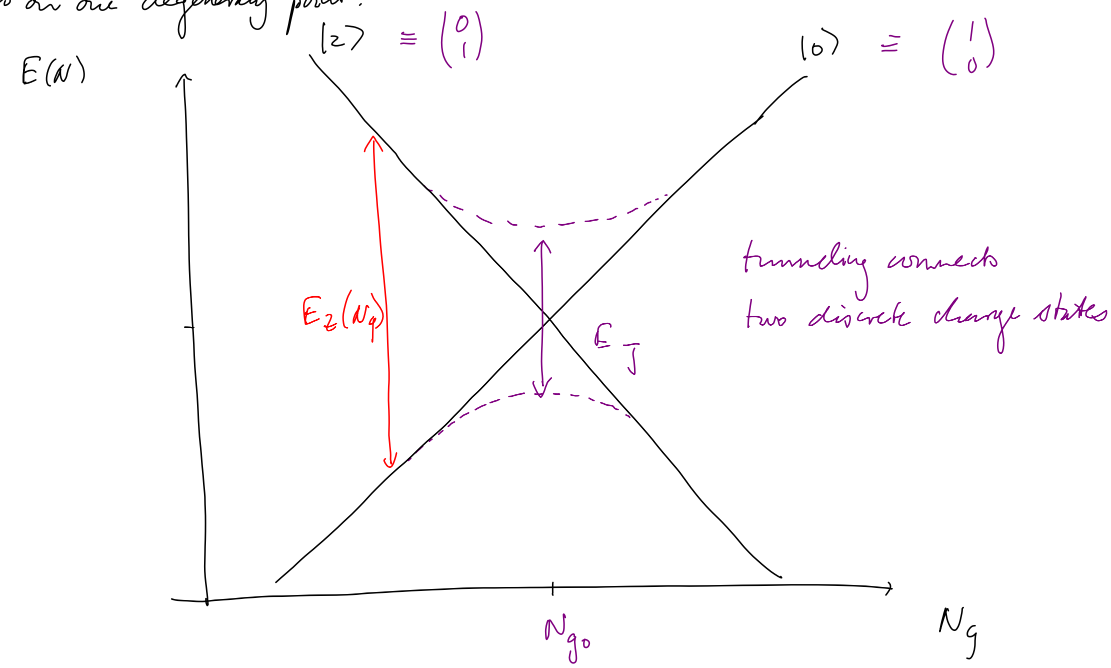

$$H_{\text{eff}} = E_z(N_g)\,\sigma_z + E_J(B)\,\sigma_x = \text{"Qubit Hamiltonian"}$$

tunable !!

Pulse protocol to observe oscillations between $|0\rangle$ and $|2\rangle$ Sec 7

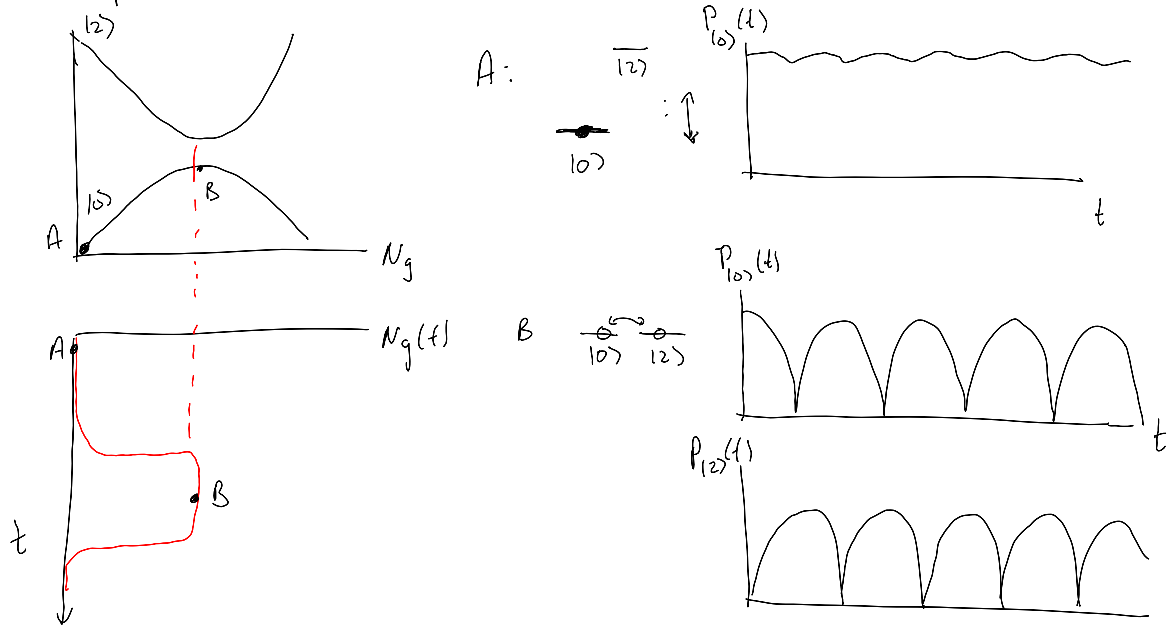

---

letters to nature, Vol 398, 786 (1999)

Sec 8

Coherent control of macroscopic quantum states in a single-Cooper-pair box

Y. Nakamura*, Yu. A. Pashkin† & J. S. Tsai*

$\Delta = 230\ \mu eV$

$E_c = 117\ \mu eV$

$E_J = 52\ \mu eV$

$k_B T = 3\ \mu eV \quad (T = 30\ mK)$

island has $N \sim 10^8$

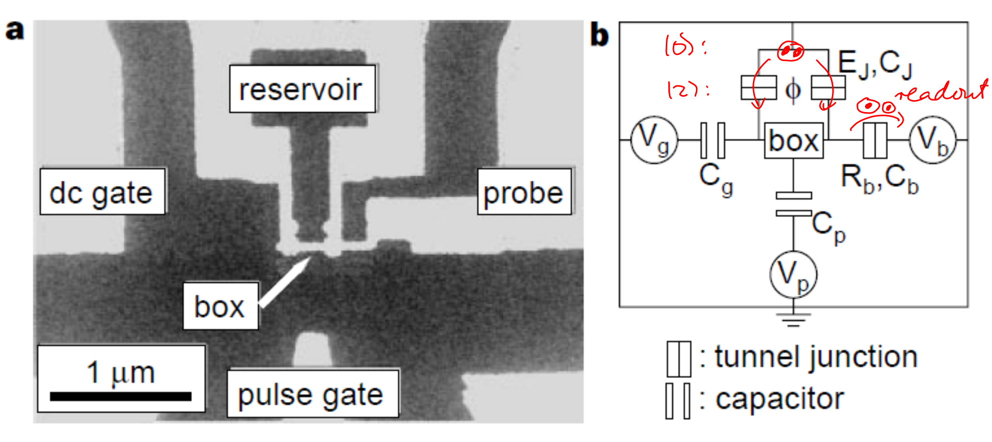

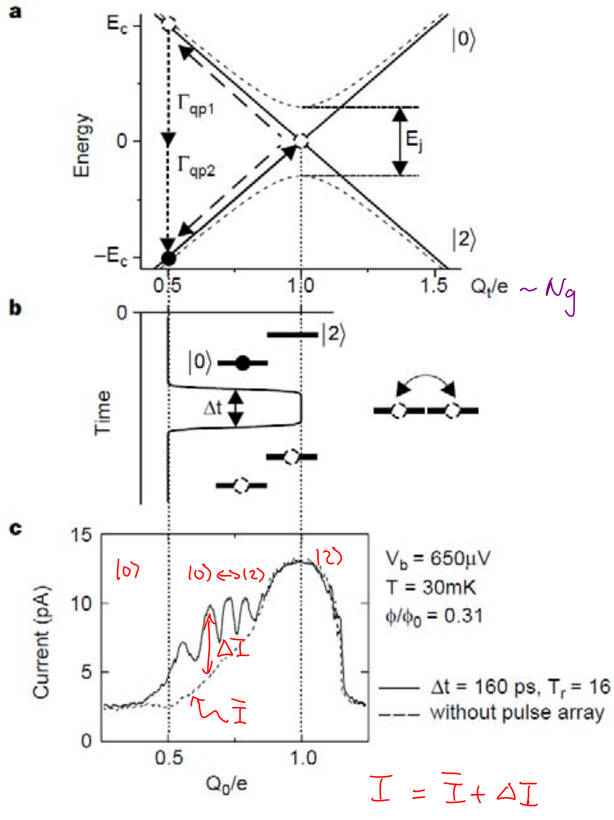

Figure 2 Pulse modulation of quantum states. **a**, Energy diagram illustrating electrostatic energies (solid lines) of two charge states $|0\rangle$ and $|2\rangle$ (with the number of excess charges in the box $n = 0$ and 2) as a function of the total gate-induced charge $Q_t = Q_0 + C_p V_p(t)$, where $Q_0 = C_g V_g + C_b V_b$ is the d.c.-gate induced charge. The dashed curves show eigenenergies (in the absence of the quasi-particle tunnelling at the probe junction) as a function of Q_t. Suppose that before a pulse occurs, Q_t equals Q_0, which is far from the resonance point, and the system is approximately in the pure charge state $|0\rangle$ (filled circle at lower left). Then, a voltage pulse of an appropriate height abruptly brings the system into resonance $Q_t/e = 1$ (solid arrow), and the state starts to oscillate between the two charge states. At the end of the pulse, the system returns to $Q_t = Q_0$ (dashed arrow) with a final state corresponding to the result of the time evolution. Finally, the $|2\rangle$ state decays to $|0\rangle$ with two quasiparticle tunnelling events through the probe junction with rates of Γ_{qp1} and Γ_{qp2} (dotted arrows). **b**, Schematic pulse shape with a nominal pulse length Δt (solid line). The rise/fall times of the actual voltage pulse was about 30–40 ps at the top of the cryostat. The voltage pulse was transmitted through a silver-plated Be-Cu coaxial cable (above 4.2 K), a Nb coaxial cable (below 4.2 K) and an on-chip coplanar line to the open-ended pulse gate shown in Fig. 1a. The insets illustrate situations of the energy levels before/during/after the pulse. **c**, Current through the probe junction versus Q_0 with (solid line) and without (dashed line) the pulse array. The pulse length was $\Delta t = 160$ ps and the repetition time was $T_r = 16$ ns. The data were taken at $V_b = 650\,\mu$V and $\phi/\phi_0 = 0.31$, where $\phi_0 = h/2e$ is a flux quantum.

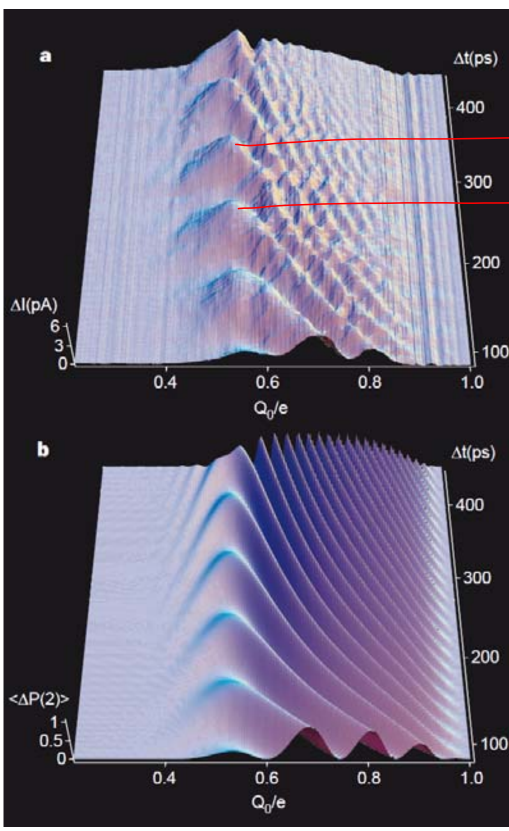

$$T_{coh} = \frac{\hbar}{E_J} \quad \text{at} \quad N_g = 1$$

$$= \frac{1}{\left[E_J^2 + E_z^2(N_g)\right]^{1/2}}$$

Figure 3 Effect of applying pulses as a function of d.c.-induced charge Q_0 and pulse length Δt. **a**, Three-dimensional plot of pulse-induced current ΔI which is the difference between currents measured with and without a pulse array. $\Delta t = 80$ ps was the shortest pulse length available with our pulse-pattern generator (Anritsu MP1758A). **b**, Calculated average increase in probability density at $|2\rangle$ after a single-pulse operation, $\langle \Delta P(2) \rangle$. The averaged probability density after the pulse was calculated by numerically solving a time-dependent Schrödinger equation and by averaging out small residual oscillations in the time domain. The effect of decoherence was not included. As the initial condition of the Schrödinger equation, we used a mixture of two eigenstates at $Q_t = Q_0$ with weights obtained from a steady-state solution of density-matrix equations that describe charge transport through the device in the absence of a pulse array. The initial probability density was also calculated from the steady-state solution. In the calculations, Josephson energy $E_J = 51.8\,\mu$eV and an effective pulse height $\Delta Q_p/e = 0.49$ were used. The solid line in Fig. 2b shows an example (at $\Delta t = 300$ ps) of the pulse shape used in this calculation.

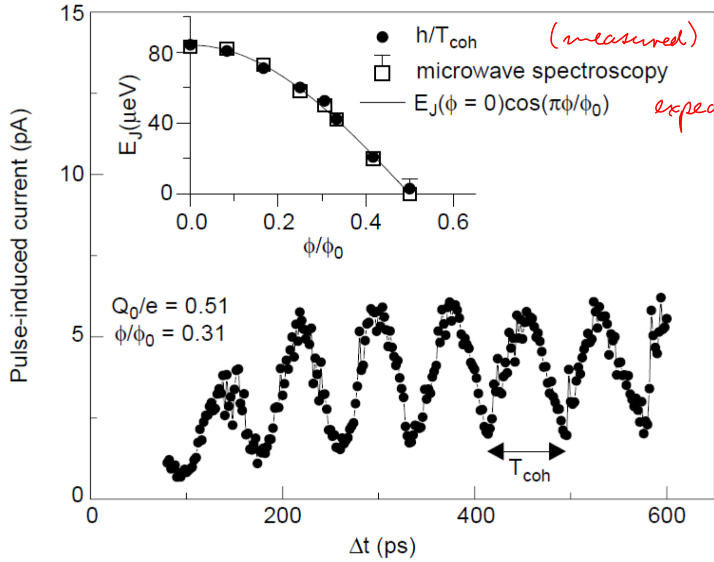

expected (tunable by magnetic field)

Figure 4 Pulse-induced current as a function of the pulse length Δt. The data correspond to the cross-section of Fig. 3a at $Q_0/e = 0.51$. Inset, Josephson energy E_J versus the magnetic flux ϕ penetrating through the loop. E_J was estimated by two independent methods. One was from the period of the coherent oscillation T_{coh} as h/T_{coh}. The other was from the gap energy observed in microwave spectroscopy[4]. The solid line shows a fitting curve with $E_J(\phi = 0) = 84\,\mu eV$ assuming cosine ϕ-dependence of E_J.